THE JOURNAL OF PHYSICAL CHEMISTRY B

Article

pubs.acs.org/JPCB

Factors Governing the Conformational Tendencies of C^{α}-Ethylated α-Amino Acids: Chirality and Side-Chain Size Effects

Jordi Casanovas,[†] Guillermo Revilla-López,[‡] Marco Crisma,[§] Claudio Toniolo,[§] and Carlos Alemán[‡,⊥,*]

[†]Departament de Química, Escola Politècnica Superior, Universitat de Lleida, 25001 Lleida, Spain

[‡]Departament d'Enginyeria Química, E. T. S. d'Enginyeria Industrial de Barcelona, Universitat Politècnica de Catalunya, 08028 Barcelona, Spain

[§]ICB, Padova Unit, CNR, Department of Chemistry, University of Padova, 35131 Padova, Italy

[⊥]Center for Research in Nano-Engineering, Universitat Politècnica de Catalunya, 08028 Barcelona, Spain

ABSTRACT: The intrinsic conformational properties of the *N*-acetyl-*N*′-methylamide derivatives of D-C^{α}-ethylglycine (Abu), D-C^{α}-methyl-C^{α}-ethylglycine (Iva), and $C^{\alpha,\alpha}$-diethylglycine (Deg) have been investigated using quantum mechanical calculations in the gas phase and in chloroform, dichloromethane and aqueous solutions. Although the large number of flexible dihedral angles results in many minimum energy conformations, only a few of them are energetically representative because of the repulsive interactions between the ethyl groups and the backbone atoms. The conformational restrictions imposed by such repulsions increase as follows: Abu < Iva < Deg. The most important characteristics of the investigated residues are as follows: (i) the conformation tendencies of Abu resemble those of standard residues with similar constitution (e.g., Val or Leu); (ii) the properties of Iva are relatively similar to those of $C^{\alpha,\alpha}$-dimethylglycine, which is the simplest $C^{\alpha,\alpha}$-dialkylated α-amino acid, even though the former is more restricted than the latter; (iii) the conformational flexibility of Deg is even lower than that of $C^{\alpha,\alpha}$-dialkylated residues with bulkier side groups (*e.g.*, $C^{\alpha,\alpha}$-diphenylglycine and $C^{\alpha,\alpha}$-dibenzylglycine).

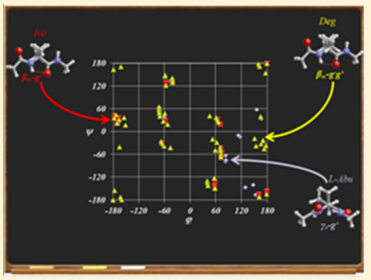

INTRODUCTION

Among synthetic noncoded residues, the conformational propensities of which can be exploited in the design of peptide analogues with well-defined backbone conformations, $C^{\alpha,\alpha}$-dialkylated glycines have attracted great attention. The simplest α-amino acid of this class is α-aminoisobutyric acid (Aib), also named $C^{\alpha,\alpha}$-dimethylglycine or C^{α}-methylalanine. In this residue, replacement of α-hydrogen atom in Ala by a methyl group results in a drastic reduction of the available conformational space. Theoretical and experimental studies[1−18] have highlighted the very strong tendency of Aib to induce folded structures in the 3_{10}-/α-helical region ($\varphi,\psi \approx \pm 60°, \pm 30°$) of the conformational space, while *semi*-extended or extended conformations are extremely rare for this residue.[4] In comparison, Ala is easily accommodated in both folded and extended structures. Thus, a local increment in the steric hindrance around the α-carbon is responsible for an effective promotion of helical arrangements in Aib-containing peptides.

On the other hand, it has been observed that symmetric $C^{\alpha,\alpha}$-dialkylated α-amino acids with both side chains bulkier than a methyl group are able to stabilize an unusual, extended secondary structure denoted 2.0_5-helix.[19−22] This helical arrangement is based on the propagation of an extended conformation that involves a five-membered intramolecularly hydrogen-bonded ring, hereafter referred to as the C_5 conformation.[23,24] The 2.0_5-helix is remarkably fragile, tending to evolve toward more compact 3D-organizations when modest changes are introduced either in the environment or in the peptide constitution.[25,26] Homo-oligopeptides based on $C^{\alpha,\alpha}$-diethylglycine (Deg, Figure 1), in which two ethyl groups are attached to the α-carbon atom, represent a classical example of this conformational behavior.

To control selectively the secondary structure of homopeptides made of symmetric $C^{\alpha,\alpha}$-dialkylated α-amino acids, the

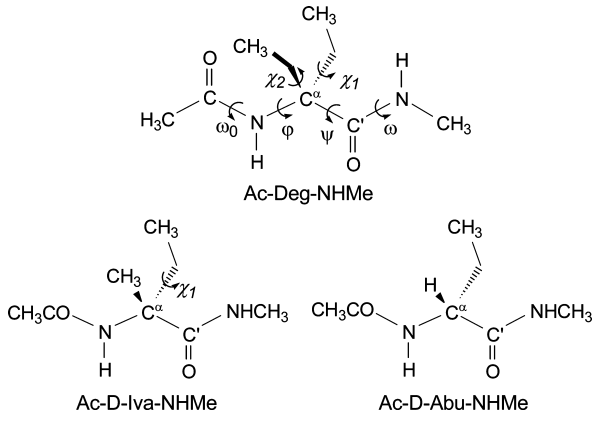

Figure 1. Chemical structures of the monopeptides investigated, Ac-Deg-NHMe, Ac-D-Iva-NHMe and Ac-D-Abu-NHMe. The backbone and side-chain dihedral angles are indicated.

Received: May 9, 2012
Revised: September 26, 2012
Published: November 5, 2012

conformational effects produced by targeted substitutions using amino acids with a chiral α-carbon atom was investigated. In particular, this idea was explored for the homopentapeptide Tfa-(Deg)$_5$-O*t*Bu (Tfa, trifluoroacetyl; O*t*Bu, *tert*-butoxy).[27] It was found that the replacement of the central Deg residue by α-aminobutyric acid (Abu, Figure 1), also named C$^\alpha$-ethylglycine, induces a symmetry disruption in the peptide chain. Interestingly, Abu critically affects the 2.0$_5$-helix adopted both in solvents of low polarity and in the crystal state by the aforementioned Deg homopentapeptide.[28−30] Specifically, Tfa-(Deg)$_2$-Abu-(Deg)$_2$-O*t*Bu folds into a 3$_{10}$-helix[31] in the crystal state, while in solution the spectroscopic information points to an increase of the population of folded conformers as compared to that of the parent homopeptide.[27]

More recently, the conformational effects of breaking the symmetry of the host Tfa-(Deg)$_5$-O*t*Bu homopentapeptide with punctual replacements at different sequence positions of one Deg residue by Abu, was examined using molecular dynamics (MD) simulations.[32] Simulations showed that only the Deg homopeptide is able to stabilize a 2.0$_5$ helix, even though a kinked arrangement with all of the Deg residues adopting an extended conformation was found to be stable when the Abu residue is introduced in the middle of the sequence. On the other hand, when the Abu residue is closer to the C-end of the sequence, the peptide chain prefers a partially folded 3$_{10}$-helix. Additional simulations on Tfa-(Deg)$_3$-Abu-(Deg)$_3$-O*t*Bu highlighted that, when the size of the Deg segments increases, their tendency to adopt a 2.0$_5$ helix predominates over the preferred folded conformation of Abu.

In spite of the potential nanotechnological applications (as spacers and switch modules) of peptides and polypeptides with conformational tendencies modulated by breaking the α-carbon symmetry of Deg, the intrinsic propensities of Deg and Abu have not been theoretically explored yet by use of *ab initio* or DFT quantum mechanical methods. Specifically, the intrinsic conformational preferences of a total of 29 C$^\alpha$-tetrasubstituted α-amino acids have been determined to date according to a literature search.[33] Analysis of these amino acids using the NCAD (non-coded aminoacids database) database[33,34] indicates that in only three of them the α- carbon is not involved in a cyclic structure, as occurs in Deg. These are Aib,[35] diphenylglycine[36] (Dϕg) and dibenzylglycine[37] (Db$_z$g). Unfortunately, the intrinsic conformational propensities of Deg cannot be directly inferred from these amino acids because of the different conformational properties of Aib[35] and the bulky aromatic side groups of Dϕg and Db$_z$g.

In this work, we present a systematic study of the intrinsic conformational preferences of the *N*-acetyl-*N*′-methylamide derivatives of Deg and D-Abu (Ac-Deg-NHMe and Ac-D-Abu-NHMe, respectively) using density functional theory (DFT) calculations. Furthermore, for the sake of completeness, the conformational study was extended to D-1-amino-2-methylbutyric acid, also named D-C$^\alpha$-ethylalanine, or D-C$^\alpha$-methyl, C$^\alpha$-ethylglycine, or D-isovaline (D-Iva, Figure 1), which was found to incorporate some of the unique structural features of Aib. A comparison of the conformational preferences obtained for Ac-Deg-NHMe, Ac-D-Abu-NHMe and the *N*-acetyl-*N*′-methylamide derivative of D-Iva (Ac-D-Iva-NHMe) provides understanding of the specific role played by both the amino acid chirality and size of the alkyl side-chain groups. Finally, a complete view of the conformational features produced by C$^{\alpha,\alpha}$-dialkylation is given by comparing the intrinsic preferences of Deg and Iva with those already reported for Aib, Dϕg, and Db$_z$g.[35−37]

METHODS

All calculations were carried out using the Gaussian 03 computer program.[38] DFT calculations were performed using the B3LYP functional[39,40] combined with the 6-31+G(d,p) basis set.[41]

The backbone ($\omega_0, \varphi, \psi, \omega$) and side-chain ($\chi_i$) dihedral angles of Ac-X-NHMe with *X* = Deg, D-Abu, and D-Iva are displayed in Figure 1. The *trans* state was considered for both ω_0 and ω in all cases since for nonproline derived α-amino acids it has been considered the most energetically favored isomer.[42−45] Because each flexible backbone and side-chain dihedral angle is expected to exhibit three minima, *i.e.*, *gauche*$^+$ (60°), *trans* (180°), and *gauche*$^-$ (−60°), the number of minima that may be anticipated for the potential energy hypersurface $E = E(\varphi,\psi,\chi_i)$ of Ac-X-NHMe with X = Deg, D-Abu and D-Iva is 3^4= 81, 3^3= 27, and 3^3= 27, respectively. All these structures were used as starting points for subsequent full geometry optimizations at the B3LYP/6-31+G(d,p) level. Frequency analyses were carried out to verify the nature of the minimum state of all the stationary points obtained and to calculate the zero-point vibrational energies (ZPVE) and both thermal and entropic corrections using the rigid-rotor harmonic oscillator approximation. These statistical terms were then used to compute the relative Gibbs free energies in the gas phase at 298 K (ΔG_{gp}). Furthermore, in order to evaluate the influence of the torsional anharmonicity in the thermochemical properties of the compounds under study, the Gibbs free energies in the gas phase at 298 K were calculated for selected conformations using the MSTor procedure that was recently developed by Truhlar and co-workers ($\Delta G_{gp(MSTor)}$).[46,47]

To obtain an estimation of the solvation effects on the relative stability of the different minima, single point calculations were conducted on the B3LYP/6-31+G(d,p) optimized structures using a Self-Consistent Reaction Field (SCRF) model. Furthermore, in order to examine the influence of solvent-induced geometry relaxation effects on the relative stability, complete geometry optimizations in solution were carried out on selected conformations. SCRF methods treat the solute at the quantum mechanical level, while the solvent is represented as a dielectric continuum. Specifically, the polarizable continuum model (PCM), developed by Tomasi and co-workers,[48−50] was used to describe the bulk solvent. This method involves the generation of a solvent cavity from spheres centered at each atom in the molecule and the calculation of virtual point charges on the cavity surface representing the polarization of the solvent. The magnitude of these charges is proportional to the derivative of the solute electrostatic potential at each point calculated from the molecular wave function. The point charges may, then, be included in the one-electron Hamiltonian, thus inducing polarization of the solute. An iterative calculation is carried out until the wave function and the surface charges are self-consistent. PCM calculations were performed using the standard protocol implemented in Gaussian 03[38] and considering the dielectric constant of chloroform (ε = 4.7), dichloromethane (ε = 8.9) and water (ε = 78.3). The conformational free energies in solution (ΔG_{chl}, ΔG_{dcm}, and ΔG_{wat}, respectively) were computed using the classical thermodynamic scheme; i.e., the free energies of solvation provided by the PCM model were added to the ΔG_{gp} values.

The minimum energy conformations of the three monopeptides studied in this work were denoted using a two-label code that specifies the (φ,ψ) backbone and (χ_i) side-chain

Table 1. Values Obtained for the Representative Dihedral Angles (in deg) of Ac-D-Abu-NHMe in the Minimum Energy Conformations and Their Corresponding Relative Energies (ΔE, in kcal/mol), Free Energies in the Gas Phase at 298 K Calculated Using the Rigid-Rotor Harmonic Oscillator Approximation (ΔG_{gp}, in kcal/mol) and Considering Torsional Anharmonicity ($\Delta G_{gp(MSTor)}$, in kcal/mol), and Free Energies in Chloroform, Dichloromethane, and Aqueous Solutions at 298 K (ΔG_{chl}, ΔG_{dcm} and ΔG_{wat}, Respectively; in kcal/mol)

conformation	φ	ψ	χ_1	ΔE	ΔG_{gp}/ $\Delta G_{gp(MSTor)}$ [a]	ΔG_{chl}	ΔG_{dcm}	ΔG_{wat}
γ_D-t	83.2	−79.4	170.4	0.0[b]	0.2/0.1	1.8	2.3	3.1
γ_D-g$^+$	83.8	−75.3	64.7	0.3	0.0/0.0[b]	1.4	1.9	2.5
β_{DL}-g$^-$	153.8	−167.3	−63.3	1.3	0.1/0.1	0.3	0.4	0.5
β_{DL}-t	147.9	−141.2	174.0	1.4	1.1/1.1	1.2	1.3	0.7
β_{DL}-g$^+$	129.5	−147.3	62.9	1.4	0.2/0.2	0.0	0.0	0.0
γ_D-g$^-$	83.4	−63.7	−55.2	1.6	1.3/1.3	4.6	5.7	6.7
γ_L-g$^+$	−72.8	55.9	60.5	2.3	2.3	2.6	2.9	3.7
γ_L-t	−73.0	62.3	172.7	2.6	2.3	2.7	2.9	3.7
α_D-g$^+$	112.8	−10.3	65.5	2.6	1.5/1.4	1.4	1.0	0.1
α_D-g$^-$	117.5	−14.2	−62.4	3.1	1.5/1.4	3.1	3.4	2.8
γ_L-g$^-$	−61.0	37.1	−74.7	5.5	5.8	5.8	5.9	6.6
δ_L-t	155.7	58.0	175.8	6.7	5.1	4.6	4.0	1.6
α_L-t	−68.1	−30.2	153.2	6.9	6.1	5.0	4.1	2.7
δ_L-g$^-$	166.8	33.3	−59.1	7.5	7.0	7.5	7.6	5.6
ε_L-g$^-$	−45.8	133.3	−55.1	9.3	9.4	9.2	9.1	9.0

[a] $\Delta G_{gp(MSTor)}$ has been calculated for the structures with $\Delta G_{gp} \leq 1.5$ kcal/mol. [b] $E = -535.215382$ au. [b] $G_{gp} = -535.041316$ au.

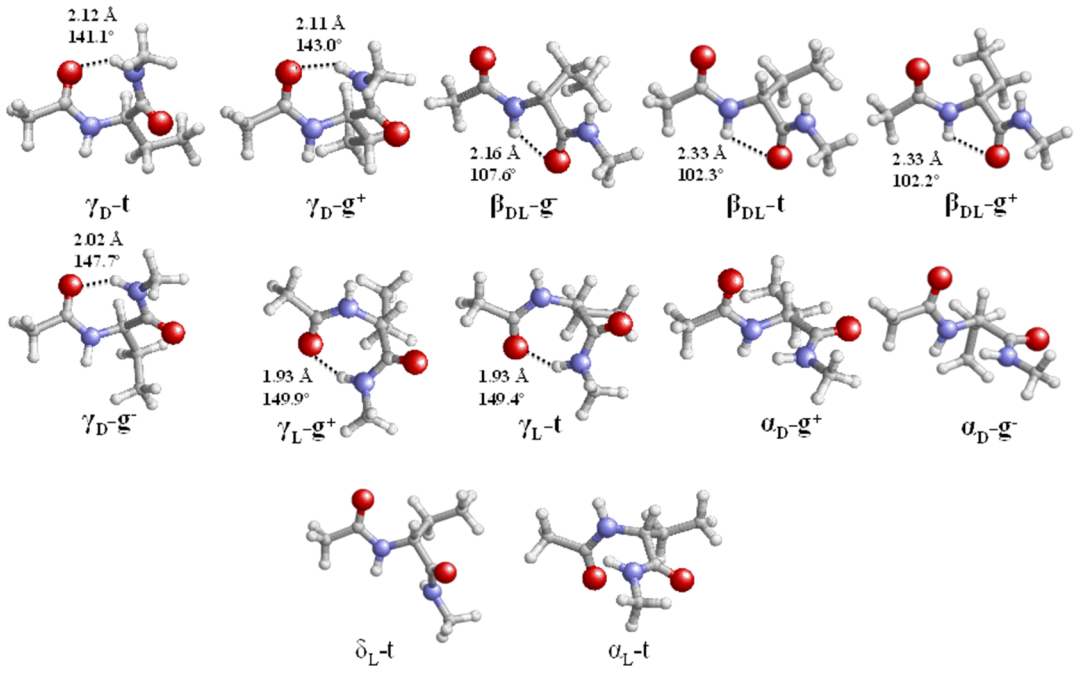

Figure 2. Molecular representations of the minimum energy structures of Ac-D-Abu-NHMe having ΔG_{gp}< 3.0 kcal/mol or ΔG_{wat}< 3.0 kcal/mol. Hydrogen bonding parameters (N−H···O distance and ∠N−H···O angle) are specified when necessary.

conformations. The first label identifies the backbone conformation using the nomenclature introduced by Perczel et al.[51] Accordingly, nine different backbone conformations can be distinguished in the potential energy surface $E = E(\varphi,\psi)$ of amino acids: γ_D, δ_D, α_D, ε_D, β_L, ε_L, α_L, δ_L, and γ_L. The second label refers to conformations of the side-chain dihedral angles (i.e., χ_1 for Ac-D-Abu-NHMe and Ac-D-Iva-NHMe, and both χ_1 and χ_2 for Ac-Deg-NHMe), which were categorized as *gauche*$^+$ (g$^+$), *trans* (t), and *gauche*$^-$ (g$^-$).

RESULTS AND DISCUSSION

Ac-D-Abu-NHMe. Geometry optimization at the B3LYP/6-31+G(d,p) level of the 27 starting geometries afforded 15 different minimum energy structures. In order to examine the influence of anharmonic modes in the thermochemical properties of these structures, the free energy of those with $\Delta G_{gp} \leq 1.5$ kcal/mol, where ΔG_{gp} refers to the free energy in the gas-phase estimated using the rigid-rotor harmonic oscillator approximation, was calculated using the MSTor methodology. The resulting values, denoted $\Delta G_{gp(MSTor)}$, are compared in Table 1 with the ΔG_{gp} values. As it can be seen, the relative free energy order was not altered by considering anharmonicity, the largest difference between the $\Delta G_{gp(MSTor)}$ and ΔG_{gp} values being of only 0.15 kcal/mol. These results indicate that thermochemical properties derived from the rigid-rotor harmonic oscillator approximation are significant enough for the compounds under

dx.doi.org/10.1021/jp3045115 | J. Phys. Chem. B 2012, 116, 13297−13307

study and, therefore, $\Delta G_{gp(MSTor)}$ has not been evaluated for the other conformers and for the other two dipeptides.

The minima visit almost all Perczel's regions with exception of two (δ_D and ε_D). This finding highlights a remarkable conformational plasticity for this noncoded α-amino acid as compared to Aib. Thus, the conformational profile of Aib, a structural isomer of D-Abu, is considerably more restricted, even though the δ_D region is represented in Ac-Aib-NHMe[35] whereas it is not detected in Ac-D-Abu-NHMe. In spite of this flexibility, the energetic accessibility of Ac-D-Abu-NHMe minima is not uniform (Table 1): eight structures show $\Delta G_{gp} \leq 1.5$ kcal/mol, two have 1.5 kcal/mol < $\Delta G_{gp} \leq 3.0$ kcal/mol, and five show $\Delta G_{gp} > 3.0$ kcal/mol, 9.4 kcal/mol being the highest value. The number of accessible backbone structures decreases when the polarity of the environment increases. Specifically, only five/four/four structures have $\Delta G_{chl}/\Delta G_{dcm}/\Delta G_{wat} \leq 1.5$ kcal/mol, three/four/four have 1.5 kcal/mol < $\Delta G_{chl}/\Delta G_{dcm}/\Delta G_{wat} \leq 3.0$ kcal/mol, and seven/seven/seven show $\Delta G_{chl}/\Delta G_{dcm}/\Delta G_{wat} >$ 3.0 kcal/mol, 9.2, 9.1, and 9.0 kcal/mol being the widest free energy gap in chloroform, dichloromethane, and water, respectively. These results point toward a reduction of the available conformational space upon solvation. Figure 2 shows the minimum energy structures with ΔG_{gp} or $\Delta G_{wat} < 3.0$ kcal/mol.

The lowest energy structure in gas phase is the γ_D-g$^+$ (Figure 2), which corresponds to a γ-turn stabilized by a seven-membered hydrogen-bonded ring.[52,53] This is not a surprising result since the stability of this structural motif is typically overestimated in the gas phase due to the lack of environmental forces (e.g., peptide···solvent interactions) competing with the intramolecular hydrogen bond. However, the β_{DL}-g$^-$ and β_{DL}-g$^+$ are destabilized in the gas phase by just 0.1 and 0.2 kcal/mol, respectively, highlighting the strong preference of Abu for the extended conformation. This feature is in clear accordance with the conformational profile of Aib in which the extended conformation was found to be strongly favored in the gas phase[35] and close in energy to the γ-turn motif. The role played by the backbone···side chain steric interactions is crucial to explain this stability. As an example, the β_{DL}-t minimum is disfavored by 1.1 kcal/mol with respect to the lowest energy conformation, this feature being attributed to the repulsive contact between the side-chain group and the backbone. The last argument is also valid to explain the 1.6 kcal/mol free energy gap between γ_D-t and γ_D-g$^-$.

Backbone helical conformations, both α_D-g$^+$ and α_D-g$^-$, present ΔG_{gp} values of 1.5 kcal/mol. It is worth pointing out that, according to the Perczel's classification, these structures are at the borderline between the γ_D and α_D regions, the former region being discarded because of the lack of the intramolecular hydrogen bond typically found in the γ-turn motif. Propagation of these helical conformations results in a left-handed helix, the only conformation able to produce a right-handed helical arrangement being the α_L-t. However, the latter minimum is destabilized by 6.1 kcal/mol because of the backbone···side-chain steric interactions induced by the chirality of Abu. The structures with the backbone dihedral angles located in the γ_L region of the conformational map are disfavored by 2.3 kcal/mol at least. This finding indicates that they are energetically inaccessible in the gas-phase at room temperature. Finally, the δ_L-t, δ_L-g$^-$, and ε_L-g$^-$ minima, which show ΔG_{gp} values of 5.1, 7.0, and 9.4 kcal/mol, respectively, illustrate the remarkable differences between the intrinsic conformational properties of Abu and its structural isomer Aib. More specifically, the δ_L backbone arrangement is not identified as a minimum in Ac-Aib-NHMe while the ε_L conformation is disfavored by only 1.4 kcal/mol in the gas phase.[35]

The PCM model of Tomasi and co-workers[48−50] was used to estimate the effect of the solvent on the relative stability of the gas-phase minima. The results are listed in Table 1. The most remarkable feature of these calculations is that β_{DL}-g$^+$ becomes the lowest energy structure in chloroform, dichloromethane and water, even though the α_D-g$^+$ shows just a 0.1 kcal/mol imbalance in aqueous solution. In contrast, the γ_D-g$^+$ conformation, which is identified as the minimum with the lowest ΔG_{gp}, is disfavored by 1.4, 1.9, and 2.5 kcal/mol in chloroform, dichloromethane and aqueous solution, respectively. The high propensity of Abu to adopt an extended conformation in polar solvents is corroborated by the low ΔG_{wat} values found for the β_{DL}-g$^-$ and β_{DL}-t structures (i.e., at 0.5 and 0.7 kcal/mol, respectively). All of the other conformers are disfavored by more than 1.5 kcal/mol.

Despite the marked tendency toward the β_{DL} backbone conformation, the α_D arrangement should be also considered as strongly representative, especially in aqueous solution, since the ΔG_{wat} of the α_D-g$^+$ minimum is 0.1 kcal/mol. The stabilization of the latter conformation is explained by the helix maximization of the molecular dipole moment, which favors solvation in water. Conformer δ_L-t, which can be considered an intermediate between the γ-turn and right-handed helical motifs, is destabilized by 4.6, 4.0, and 1.6 kcal/mol in chloroform, dichloromethane, and aqueous solution, respectively (i.e., this represents a narrowing in the free energy gap of 0.5, 1.1, and 3.5 kcal/mol, respectively, with respect to the gas phase). The propensity of Abu for helix-like conformations in polar solvents was identified when this amino acid was embedded in the short homopeptide made of Deg residues.[32] More specifically, we observed that Abu has a strong tendency to disrupt the well-defined preference of Deg toward extended conformations in favor of kinked arrangements. On the other hand, the backbone γ_D and γ_L conformations are disfavored in aqueous solution by at least 2.5 and 3.7 kcal/mol, respectively. This finding represents a drastic reduction in their accessibility with respect to the gas phase. In summary, a comparison among the ΔG_{wat}, ΔG_{dcm}, ΔG_{chl}, and ΔG_{gp} values displayed in Table 1 clearly indicates that the stability of the conformers in solution is influenced not only by steric interactions but also by the polar components of the backbone, the importance of the role by the latter increasing with the polarity of the solvent.

The differences in the conformational preferences of Ac-D-Abu-NHMe in the gas phase and in solution discussed above are illustrated in Figure 3a, which shows the position of the most favored structures in the φ,ψ-map. Moreover, the φ,ψ values of Abu residues in crystallized peptides are included in the same Figure. To this purpose, we identified a total of eight structures of Abu-containing derivatives and linear peptides from those reported in the Cambridge Structural Database (CSD, version 5.33, November 2011)[54] and in ref 27. In our statistical analysis, the X-ray diffraction structures of the free amino acid itself, the few linear peptides where Abu is positioned at the N-terminus and not acylated (in such cases the φ torsion angle is not defined), and a number of cyclic peptides where the Abu conformation might be biased by the ring system were not considered representative. Among the 12 Abu residues (taking into account the crystallographically independent molecules), three are helical, four *semi*-extended, and five extended. As it can be seen, our theoretical predictions are in good agreement with the crystal-state experimental information. It is also worth

dx.doi.org/10.1021/jp3045115 | J. Phys. Chem. B 2012, 116, 13297−13307

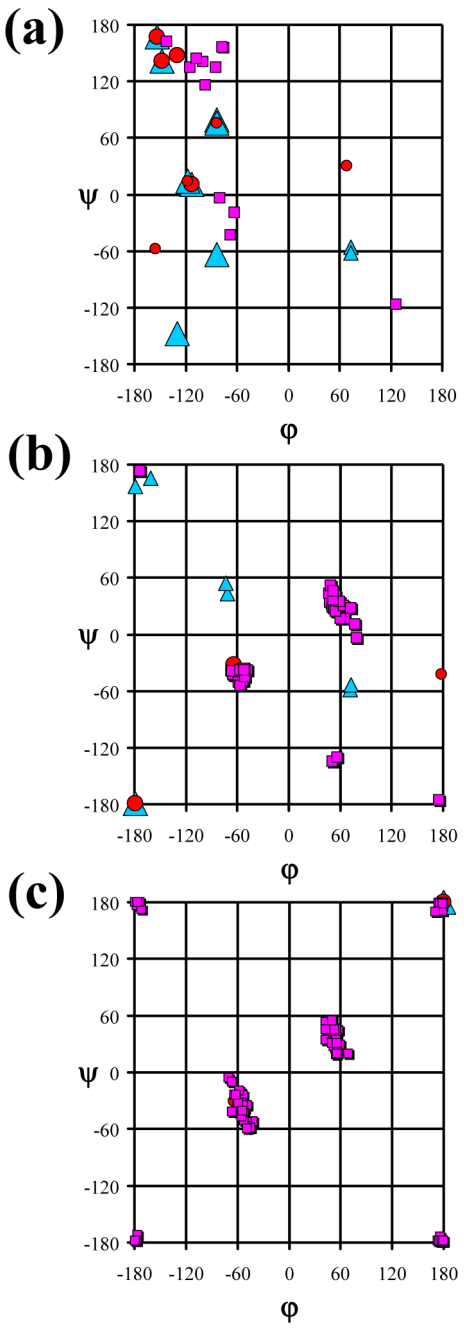

Figure 3. Representative minimum energy structures in the gas phase and aqueous solution calculated for (a) Ac-L-Abu-NHMe, (b) Ac-L-Iva-NHMe and (c) Ac-Deg-NHMe. The structures with $\Delta G_{gp} \leq 1.5$ and 1.5 kcal/mol < $\Delta G_{gp} \leq 3.0$ kcal/mol are represented by large and small blue triangles, respectively, while those with $\Delta G_{wat} \leq 1.5$ and 1.5 kcal/mol < $\Delta G_{wat} \leq 3.0$ kcal/mol correspond to the large and small red circles, respectively. Pink squares represent the positions in the φ,ψ-map of Abu, Iva and Deg residues contained in crystallized peptides. In order to avoid misinterpretation of the results because of the chirality of Abu and Iva, all of the structures of Ac-Abu-NHMe and Ac-Iva-NHMe have been represented in the map considering the L-Abu and L-Iva enantiomer, respectively (i.e., the signs of all dihedral angles have been changed with respect to Tables 1 and 2).

pointing out that some of us (M.C. and C.T.) have found that the longest Abu homo-oligomers synthesized exhibit a remarkable tendency to fold in solvents of low polarity, whereas in more polar solvents and in aqueous mixtures they tend to populate extended, self-associated conformations.[55] Not surprisingly, the overall conformational preferences of Abu are similar to those featured by protein amino acids with a similar side-chain constitution (*e.g.*, Val, Ile, or Leu).[56−61]

Ac-D-Iva-NHMe. B3LYP/6-31+G(d,p) geometry optimizations of the 27 starting conformations led to 19 minima, which are widely distributed, occupying all Perczel's regions with exception of δ_D. Table 2 compares their dihedral angles, relative energies and relative free energy values, while the more representative minima of this monopeptide are displayed in Figure 4. Inspection of the ΔG_{gp} values reveals that the number of structures with $\Delta G_{gp} \leq 1.5$ kcal/mol, 1.5 kcal/mol < $\Delta G_{gp} \leq 3.0$ kcal/mol, and $\Delta G_{gp} > 3.0$ kcal/mol is one, six, and 11, respectively, the largest ΔG_{gp} value being 8.4 kcal/mol. These results clearly show that the energetically accessible conformational space of Iva is very restricted in comparison to that of Abu, even though the number of minima is ∼25% higher for the former than for the latter. In both chloroform and dichloromethane this distribution changes to one, one and 17 structures with $\Delta G_{chl}\Delta G_{dcm} \leq 1.5$ kcal/mol, 1.5 kcal/mol < $\Delta G_{chl}\Delta G_{dcm} \leq 3.0$ kcal/mol, and $\Delta G_{chl}\Delta G_{dcm} > 3.0$ kcal/mol, respectively. Finally, in water the number of structures with $\Delta G_{wat} \leq 1.5$ kcal/mol, 1.5 kcal/mol < $\Delta G_{wat} \leq 3.0$ kcal/mol, and $\Delta G_{wat} > 3.0$ kcal/mol is 2, 1, and 16, respectively. These results indicate that the restricted conformational profile is preserved in these environments as well.

In the gas phase, β_{DL}-g$^-$ is the lowest energy minimum, the free energy gap with respect to the second minimum, γ_L-t, being 1.9 kcal/mol. This feature indicates that Iva has a clear preference for the extended conformation, which makes a difference with respect to Abu in which the γ-turn motif is significantly represented. An explanation for this structural difference is the increased steric hindrance of Iva: the replacement of the α-hydrogen by a methyl favors backbone arrangements that minimize the contacts between the side chains and the main chain. This hypothesis is supported by the fact that the two other β_{DL} structures, β_{DL}-t and β_{DL}-g$^+$, are 2.5 and 3.0 kcal/mol higher than the global minimum, respectively, and present the aforementioned contacts (Figure 4). A similar behavior was observed for the Aib/Dϕg/Db$_z$g series, where the tendency for the extended conformations increases with the size of the side chains.[35−37] Remarkably, at variance with Abu, the γ_L conformations (γ_L-t, γ_L-g$^+$, and γ_L-g$^-$ with ΔG^{gp} 1.9, 2.0, and 4.8 kcal/mol, respectively) are slightly preferred with respect to the γ_D conformations (γ_D-g$^-$, γ_D-g$^+$, and γ_D-t with ΔG^{gp} 2.3, 2.5, and 3.2 kcal/mol, respectively). Again, this change can be attributed to the steric tensions induced by the additional methyl group.

Helical conformations, α_D-t, α_D-g$^+$, and α_L-t are disfavored by 4.1, 4.3, and 5.7 kcal/mol, respectively. These data suggest that the accessibility to these motifs is lower for Iva than for Abu. The decrease in stability of the helical backbones is in agreement with the reported data for Aib, Dϕg, and Db$_z$g.[35−37] Indeed, the α-helical motif is disfavored by about 2.9 and 4.1 kcal/mol in Ac-Aib-NHMe and Ac-Dϕg-NHMe, respectively, whereas it is not identified as a minimum energy conformation in Ac−Db$_z$g-NHMe. Backbone conformations considered as intermediates between helical and turn motifs (i.e., ε_D-g$^+$, ε_L-g$^+$, ε_D-g$^-$, ε_L-g$^-$, δ_L-t, δ_L-g$^-$, and δ_L-g$^+$) show $\Delta G^{gp} \geq 4.2$ kcal/mol. Comparison with the ΔG^{gp} values displayed in Table 1 reveals that such intermediate conformations are significantly more stable for Iva than for Abu in the gas phase.

dx.doi.org/10.1021/jp3045115 | J. Phys. Chem. B 2012, 116, 13297−13307

Table 2. Values for the Representative Dihedral Angles (in deg) of Ac-D-Iva-NHMe in the Minimum Energy Conformations and Their Corresponding Relative Energies (ΔE, in kcal/mol), Free Energies in the Gas Phase at 298 K (ΔG_{gp}, in kcal/mol), and Free Energies in Chloroform, Dichloromethane, and Aqueous Solutions at 298 K (ΔG_{chl}, ΔG_{dcm}, and ΔG_{wat}, Respectively; in kcal/mol)

conformation	φ	ψ	χ_1	ΔE	ΔG_{gp}	ΔG_{chl}	ΔG_{dcm}	ΔG_{wat}
β_{DL}-g$^-$	179.4	179.5	−59.0	0.0[a]	0.0[b]	0.0	0.0	0.7
γ_L-t	−71.7	58.2	−178.6	0.5	1.9	3.2	3.8	4.1
γ_L-g$^+$	−72.6	53.3	59.0	0.5	2.0	3.1	3.7	4.4
γ_D-g$^-$	71.4	−42.9	−58.9	0.6	2.2	4.4	5.2	6.9
γ_D-g$^+$	73.9	−53.9	65.0	1.3	2.5	3.6	4.1	5.2
γ_D-t	72.3	−68.5	172.4	1.3	3.2	3.8	4.1	5.3
β_{DL}-t	179.4	−156.5	−178.7	1.8	2.5	3.1	3.5	4.3
β_{DL}-g$^+$	161.1	−165.1	66.4	3.0	3.0	3.7	3.9	4.7
α_D-t	63.8	32.2	−179.4	3.3	4.1	2.8	1.9	0.0
ε_L-g$^+$	−56.8	129.1	57.9	3.4	4.4	4.3	4.3	3.9
ε_D-g$^+$	58.0	−131.9	63.8	3.5	4.2	4.3	4.4	5.0
α_D-g$^+$	70.5	19.1	66.1	3.5	4.3	4.2	4.1	4.0
γ_L-g$^-$	−58.7	30.0	−74.3	3.6	4.8	6.3	6.9	7.2
ε_D-g$^-$	56.7	−142.7	−57.5	4.2	5.3	6.3	6.2	7.3
δ_L-g$^-$	−170.8	24.4	−53.7	4.8	5.7	5.5	5.5	3.9
α_L-t	−65.4	−30.0	164.7	4.9	5.7	4.6	3.9	3.1
δ_L-t	−177.8	42.1	−172.6	5.2	5.6	4.7	4.3	2.6
ε_D-g$^-$	−41.6	133.2	−51.6	6.4	7.8	8.2	8.3	7.9
δ_L-g$^+$	−167.5	37.0	99.6	8.0	8.3	7.3	6.9	5.6

[a] E = −574.528505 au. [b] G_{gp} = −574.329797 au.

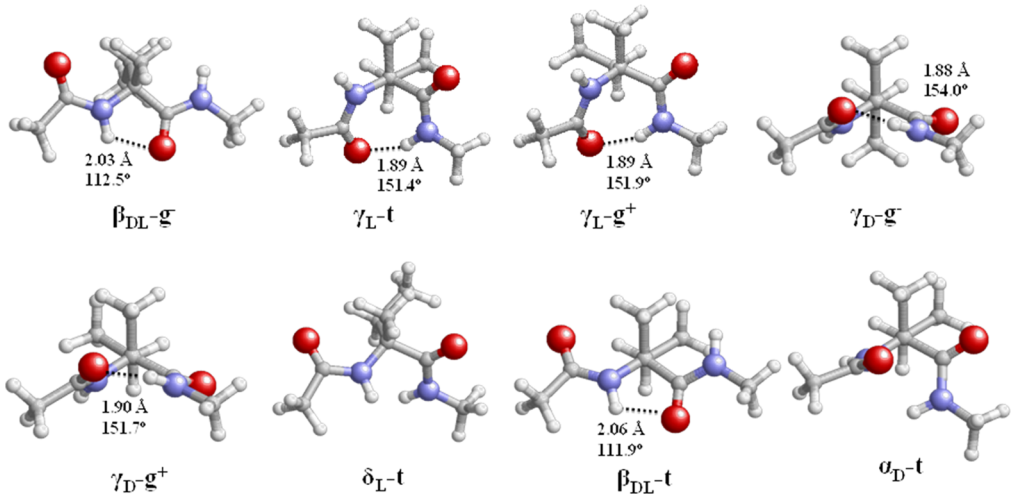

Figure 4. Molecular representations of the minimum energy structures of Ac-D-Iva-NHMe having ΔG_{gp}< 3.0 kcal/mol or ΔG_{wat}< 3.0 kcal/mol. Hydrogen bonding parameters (N−H···O distance and ∠N−H···O angle) are specified when necessary.

The ∠N−C$^\alpha$−C(=O) bond angle of the lowest energy minimum in the gas phase, β_{DL}-g$^-$, is 104.3°, evidencing a reduction of 5.2° with respect to the standard tetrahedral value. However, analysis of this geometric effect reveals a dependence on the conformation. Thus, it has been detected in the extended β_{DL} conformations only (e.g., the ∠N−C$^\alpha$−C(=O) angle of the β_{DL}-t and β_{DL}-g$^+$ conformations is 103.6° and 103.5°, respectively), the angle measured for the other backbone arrangements being closer to the standard value (e.g., for the γ_L-t and α_D-t conformations the ∠N−C$^\alpha$−C(=O) angle is 111.1° and 111.2°, respectively). Inspection of the ∠N−C$^\alpha$−C(=O) bond angles found for the minimum energy conformations of Ac-D-Abu-NHMe evidence that the reduction observed in the β_{DL} conformations of Ac-D-Iva-NHMe is consequence of the strain induced by α,α-dialkylation. Thus, the values measured for the γ_D-g$^+$, β_{DL}-g$^-$, γ_D-t, β_{DL}-g$^+$, β_{DL}-t, γ_D-g$^-$, α_D-g$^+$, and α_D-g$^-$ conformations of Ac-D-Abu-NHMe, which are all the minima with $\Delta G_{gp} \leq$ 1.5 kcal/mol, are 110.0°, 107.2°, 109.4°, 107.6°, 106.8°, 111.9°, 113.7°, and 113.6°, respectively.

Single point calculations in chloroform and dichloromethane indicate that the β_{DL}-g$^-$ is also the most favored conformation in organic solvents of low polarity. However calculations in water show significant variations in the preferred conformational profile since α_D-t becomes the lowest energy conformation, even though the β_{DL}-g$^-$ structure is destabilized by 0.7 kcal/mol only. Thus, the stability of α_D-t increases with the polarity of the environment, being unfavored with respect to the β_{DL}-g$^-$ by 4.1, 2.8, and 1.9 kcal/mol in the gas phase, chloroform, and dichloromethane, respectively. This behavior represents a significant change with respect to that of Ac-D-Abu-NHMe, which in aqueous solution shows the highest preference for the extended arrangement. Thus, the dipole moment of the helical motif, larger for Ac-D-Iva-NHMe than for Ac-D-Abu-NHMe, stabilizes this backbone arrangement. On the other hand, turn-

dx.doi.org/10.1021/jp3045115 | J. Phys. Chem. B 2012, 116, 13297−13307

Table 3. Values for the Representative Dihedral Angles (in deg) of Ac-Deg-NHMe in the Minimum Energy Conformations and Their Corresponding Relative Energies (ΔE, in kcal/mol), Free Energies in the Gas Phase at 298 K (ΔG_{gp}, in kcal/mol), and Free Energies in Chloroform, Dichloromethane, and Aqueous Solutions at 298 K (ΔG_{chl}, ΔG_{dcm} and ΔG_{wat}, Respectively; in kcal/mol)

conformation[a]	φ	ψ	χ_1	χ_2	ΔE	ΔG_{gp}	ΔG_{chl}	ΔG_{dcm}	ΔG_{wat}
β_{DL}-g$^-$g$^+$	180.0	180.0	−59.3	59.3	0.0[b]	0.0[c]	0.0	0.0	0.0
γ-g$^-$g$^-$	71.0	−41.2	−60.2	−57.7	1.8	3.5	5.8	6.7	8.2
γ-tg$^-$	70.7	−48.0	177.9	−56.5	1.8	3.9	6.4	7.2	8.8
γ-tg$^+$	72.6	−57.8	−179.0	66.6	2.0	3.9	5.3	5.9	6.8
β_{DL}-tg$^+$	179.1	−164.5	178.3	55.8	2.1	3.7	4.5	4.9	5.3
β_{DL}-g$^+$g$^+$	161.8	−171.8	63.7	59.3	3.2	4.4	4.3	4.2	4.8
γ-g$^-$g$^+$	52.6	−19.4	−63.1	69.6	4.0	5.6	7.4	8.0	9.0
ε-g$^-$t	56.8	−122.3	−61.1	179.0	4.0	5.0	5.1	5.2	4.6
α-tg$^-$	64.5	30.9	178.4	−60.7	4.2	5.4	4.2	3.6	1.8
γ-tt	71.5	−60.8	159.3	170.7	4.5	7.2	8.0	8.5	9.1
γ-g$^+$g$^-$	71.7	−49.9	66.2	−37.3	4.9	7.2	8.2	8.8	9.6
δ-g$^-$g$^+$	−170.7	22.0	−53.8	57.1	4.99	6.6	7.4	7.7	6.4
γ-g$^+$g$^+$	62.6	−28.0	66.3	82.1	5.39	7.0	8.7	9.4	11.0
ε-g$^-$g$^-$	58.3	−149.0	−57.6	−48.8	5.6	6.8	7.6	7.8	7.3
δ-tg$^+$	−177.2	36.6	−174.8	51.7	5.7	6.9	6.9	6.8	5.1
β_{DL}-tg$^-$	−162.4	−172.1	176.1	−65.4	6.1	7.2	8.1	8.5	9.2
β_{DL}-g$^+$t	162.4	172.1	65.4	−176.1	6.1	7.2	8.1	8.5	9.2
α-tg$^+$	46.1	42.1	−178.1	55.8	6.3	8.1	6.9	6.3	4.6
δ-g$^-$g$^-$	−151.2	17.8	−60.9	−64.3	6.6	8.1	7.6	7.4	6.1
α-g$^+$g$^-$	67.0	25.0	67.7	−36.3	6.9	8.3	7.6	7.4	6.1
ε-g$^-$g$^+$	58.7	−146.6	−36.1	65.0	7.1	8.9	8.2	8.1	7.8
γ-tg$^+$	59.4	−48.8	167.2	62.5	7.1	9.2	10.8	11.4	11.6
ε-tt	176.4	154.4	160.0	158.2	7.1	8.6	9.7	10.3	11.7
ε-g$^+$t	40.6	−129.1	48.4	180.0	7.1	9.2	9.0	8.9	8.7
δ-g$^-$t	−169.6	24.4	−51.5	−170.2	7.3	8.9	9.1	9.2	7.8
δ-tg$^-$	−154.2	37.2	−174.8	−67.0	7.5	8.3	7.1	6.8	5.7
α-tt	61.1	37.5	−156.8	−166.2	7.8	9.6	7.9	7.0	5.3
ε-g$^+$g$^+$	41.1	−134.2	60.4	52.2	8.3	10.1	10.9	11.2	11.6
δ-g$^+$g$^+$	−166.1	31.7	99.6	54.9	8.5	9.2	9.8	10.0	8.1
δ-g$^-$g$^+_{(II)}$	42.0	−142.0	−59.1	55.8	8.6	10.3	10.9	11.0	10.3
β_{DL}-g$^+$g$^-$	−160.2	−179.2	97.6	−45.8	8.8	10.3	10.3	10.5	10.5
δ-tt	−173.4	44.4	−152.9	−170.5	9.0	10.3	8.9	8.5	7.1
δ-g$^+$g$^-$	164.9	39.9	46.3	−96.2	14.6	16.4	16.6	16.1	15.1

[a]The subindexes "D" and "L" have been deleted from the labeling of the minima because of the achiral nature of Deg. Thus, minima with $(\varphi,\psi,\chi_1,\chi_2)$ and $(-\varphi,-\psi,-\chi_1,-\chi_2)$ are energetically degenerated and, therefore, the following equivalences have been applied: $\alpha_D \equiv \alpha_L \equiv \alpha$, $\gamma_D \equiv \gamma_L \equiv \gamma$, $\delta_D \equiv \delta_L \equiv \delta$, and $\varepsilon_D \equiv \varepsilon_L \equiv \varepsilon$, while β_{DL} remains the same. [b]E= −574.528505 au. [c]G_{gp} = −574.329797 au.

like conformations, like γ_L (e.g., γ_L-t, γ_L-g$^+$, and γ_L-g$^-$) and γ_D (e.g., γ_D-g$^+$, γ_D-t, and γ_D-g$^-$), are even more energetically disfavored in solution than in the gas phase, this feature being independent of the solvent.

Remarkable conformational changes introduced by the substitution of the α-hydrogen of Ac-D-Abu-NHMe with a methyl group in Ac-D-Iva-NHMe are observed. In particular, a comparison of the maps shown in Figure 3, parts a and b, indicates that the methyl group of Iva induces not only a drastic reduction of the conformational flexibility but also a pronounced variation of the position of the minima in both gas phase and aqueous solution.

Interestingly, some of us (M.C. and C.T.) recently performed a survey in the CSD of the X-ray diffraction structures of Iva-containing amino acid derivatives and linear peptides,[62] which returned 119 occurrences of Iva residues in 49 crystal structures. The results indicate that Iva overwhelmingly prefers helical conformations. Indeed, only two examples of the extended conformation are documented, namely the two independent molecules of mClAc-D-Iva−OH (mClAc, monochloroacetyl),[63] and two examples of the *semi*-extended conformation, namely the N-terminal residue of *p*BrBz-(D-Iva-L-Iva)$_2$-O*t*Bu (*p*BrBz, *para*-bromobenzoyl; O*t*Bu, *tert*-butoxy),[64] as it occupies the *i*+1 corner position in a type-II′ β-turn with ϕ,ψ = 57°, −130°, and the C-terminal residue of *p*BrBz-(D-Iva)$_8$-O*t*Bu (ϕ,ψ = 51°, −135°).[65] The observation that Iva almost exclusively adopts helical conformations in crystalline peptides is in good agreement with the quantum mechanical predictions in aqueous solution. Thus, the extended conformation predicted in the gas phase for the Iva monopeptide becomes severely destabilized when this amino acid is flanked by other amino acids. The remarkable tendency of Iva to adopt helical structures is similar to that reported for Aib.[35] Indeed, although quantum mechanical calculations on Ac-Aib-NHMe predict that the extended conformation is the most stable in the gas phase,[35,36] this structure is very rare when Aib is inserted in a peptide.[1−18] Further support to this analysis comes from the published conformational data on Iva homo- and host/guest peptides.[66−68] Specifically, these studies indicate that this residue exerts a strong helix-inducing effect, comparable to that shown by Aib.

Ac-Deg-NHMe. The number of starting conformations anticipated for the potential energy hypersurface E =

dx.doi.org/10.1021/jp3045115 | J. Phys. Chem. B 2012, 116, 13297−13307

$E(\varphi,\psi,\chi_1,\chi_2)$ of this monopeptide (Figure 1) is $3^4 = 81$. However, due to the absence of chirality in the Deg residue, the number of theoretical minima can be reduced to 41, since structures with $(\varphi,\psi,\chi_1,\chi_2)$ and $(-\varphi,-\psi,-\chi_1,-\chi_2)$ are energetically degenerated and equivalent. Energy minimization of such 41 starting conformations led to 33 minimum energy conformations, which are listed in Table 3. In order to reflect the degeneracy of the minima, the Perczel's regions were identified by a Greek letter only (i.e., the subindexes "D" and "L" were deleted because the achiral nature of Deg produces the following equivalences: $\alpha_D \equiv \alpha_L$, $\gamma_D \equiv \gamma_L$, $\delta_D \equiv \delta_L$ and $\varepsilon_D \equiv \varepsilon_L$, while β_{DL} remains the same). The 2-fold degenerated nature of all these minima reflects a remarkable expansion of the conformational profile with respect to those of Ac-D-Abu-NHMe and Ac-D-Iva-NHMe. Thus, the high number of minima identified for Ac-Deg-NHMe suggests that this amino acid residue may be able to accommodate in many secondary structures depending on the particular chemical environment.

The 33 minima listed in Table 3 are distributed in the following way: one minimum with $\Delta G_{gp} \leq 1.5$ kcal/mol, while the remaining 32 show $\Delta G_{gp} \geq 3.5$ kcal/mol. This unexpected feature indicates that Deg is an extremely restricted amino acid despite of the very high number of identified minima. Obviously, the main reason for this restriction is the steric hindrance introduced by the two ethyl side-chain groups, which increases the energy gap between the lowest energy conformer (i.e., the one that best accommodate the side chains) and the rest of the conformers. Similarly, in chloroform and dichloromethane only one minimum present ΔG_{chl},$\Delta G_{dcm} \leq 1.5$ kcal/mol, while the remaining 32 show ΔG_{chl},$\Delta G_{dcm} \geq 3.5$ kcal/mol, and the number of representative structures with $\Delta G_{wat} \leq 1.5$ kcal/mol, 1.5 kcal/mol $< \Delta G_{wat} \leq 3.0$ kcal/mol, and $\Delta G_{wat} > 3.0$ kcal/mol is 1, 1, and 31, respectively. Thus, the initial conformational flexibility of the amino acid provided by the high number of minima is only apparent from an energetic point of view also in aqueous solution. Figure 5 depicts the two only structures that are representative in the gas phase or in aqueous solution.

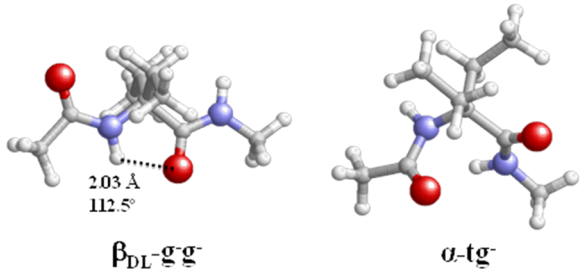

Figure 5. Molecular representations of the minimum energy structures of Ac-Deg-NHMe having $\Delta G_{gp} < 3.0$ kcal/mol or $\Delta G_{wat} < 3.0$ kcal/mol. Hydrogen bonding parameters (N−H···O distance and ∠N−H···O angle) are specified when necessary.

The backbone conformations of the minimum energy structures identified for Ac-Deg-NHMe are categorized as follows: six β_{DL}, eight γ, four α, six ε, and nine δ. Although all of the regions of the conformational map would be visited by those minima, they spread over a ΔG_{gp} interval of 16.4 kcal/mol. The preferred conformation in the gas phase is the β_{DL}-g^-g^+, which minimizes the steric contacts between the side chains and the main chain. Indeed, assuming a Maxwell−Boltzmann's probability distribution, this is the only representative and accessible structure in the gas phase (i.e., the second minimum, γ-g^-g^-, is destabilized by 3.5 kcal/mol). Interestingly, the only two types of backbone arrangements identified with ΔG_{gp} lower than 5 kcal/mol are the β_{DL} type, which in addition to the global minimum presents β_{DL}-g^+g^+ with ΔG_{gp}= 4.4 kcal/mol, and the γ type, which in addition to the second minimum shows γ-tg^+ and γ-tg^- both with ΔG_{gp}= 3.9 kcal/mol. The most favored helical conformation, α-tg^-, is destabilized by 5.4 kcal/mol.

The influence of α,α-dialkylation in the ∠N−C^α−C(=O) bond angle of Ac-Deg-NHMe is similar to that discussed above for Ac-D-Iva-NHMe, showing a dependence on the backbone conformation. However, in Ac-Deg-NHMe the geometric distortion with respect to the standard tetrahedral value occurs not only for the extended β_{DL} backbone conformation but also for the γ turn-like arrangement, the deviation with respect 109.5° being of approximately −5° and +4° for the former and the latter, respectively. For example, the ∠N−C^α−C(=O) angle measured for the β_{DL}-g^-, γ-g^-g^-, and α-tg^- conformations is 104.3°, 113.5°, and 110.9°, respectively.

Single-point calculations in chloroform, dichloromethane and aqueous solutions show that the β_{DL}-g^-g^+ is the preferred conformation also in this condensed phase. This result is fully consistent with the conformational features extracted from MD simulations of Deg-containing homopeptides in chloroform solution.[32] The second conformation in aqueous solution is $\alpha_D tg^-$, even though it is disfavored by 1.8 kcal/mol. This structure is unfavored by 5.4, 4.2, and 3.6 kcal/mol in the gas phase, chloroform solution and dichloromethane solution, respectively. This is another remarkable difference between the conformational propensities displayed by Deg and those discussed for Abu and Iva, in that the helical and *semi*-extended conformations are essentially isoenergetic for the two latter chiral amino acids. The other 31 calculated structures for Ac-Deg-NHMe show ΔG_{wat} values comprised between 4.6 and 15.1 kcal/mol.

Our statistical survey on 30 CSD and unpublished X-ray diffraction structures from the Padova laboratory of Deg-containing derivatives and linear peptides (giving a total of 91 Deg residues) shows that 61 (67%) residues are helical and 30 (33%) extended. As partially anticipated in the Introduction, from solution conformational investigations it turns out that Deg homopeptides can adopt either the extended conformation in solvents of low polarity or a helical structure in more polar solvents.[25,26,29,30,69] Thus, Figure 6c clearly shows the conformational preferences predicted for the dipeptide by quantum mechanics perfectly match the experimental observations in crystallized peptides.

Figure 6 compares the position in the φ,ψ-map of the representative minimum obtained for Ac-Deg-NHMe with those calculated at the same theoretical level for the *N*-acetyl-*N*′-methylamide derivatives of other C^α-tetrasubstituted α-amino acids: Ac-Aib-NHMe,[35,36] Ac-Dϕg-NHMe,[36] and Ac−Db$_z$g-NHMe.[37] Clearly, replacement of the two α-methyl groups (Aib) by ethyl groups (Deg) induces very remarkable conformational restraints to the backbone. Thus, Ac-Aib-NHMe shows two minimum energy structures with $\Delta G_{gp} \leq 1.5$ kcal/mol, which correspond to the extended (φ,ψ = 180.0°, 180.0°,[19−22] with ΔG_{gp} = 0.0 kcal/mol) and γ-turn (φ,ψ = −72.9°, 55.4° with ΔG_{gp} = 0.7 kcal/mol) motifs, and the helical (φ,ψ = −69.3°, −21.6°) and *semi*-extended (φ,ψ = −57.6°, 126.2°) arrangements with ΔG_{gp} values of 2.9 and 3.0 kcal/mol, respectively.[35,36] All these backbone conformations, with exception of the extended arrangement, become significantly disfavored when the α-ethyl

dx.doi.org/10.1021/jp3045115 | J. Phys. Chem. B 2012, 116, 13297−13307

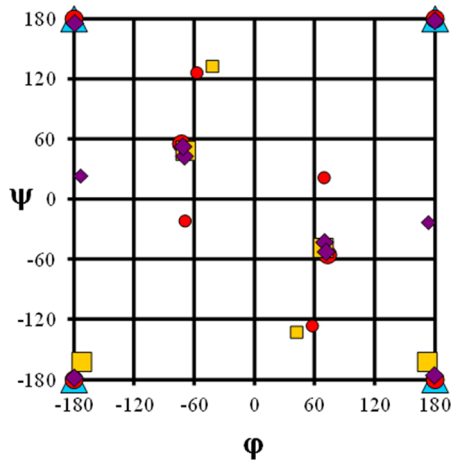

Figure 6. Representative minimum energy structures calculated for (a) Ac-Deg-NHMe (blue triangles), (b) Ac-Aib-NHMe (red circles), (c) Ac-Dϕg-NHMe (yellow squares), and (d) Ac−Db$_z$g-NHMe (purple diamonds). The structures with $\Delta G_{gp} \leq$ 1.5 and 1.5 kcal/mol < $\Delta G_{gp} \leq$ 3.0 kcal/mol are represented by large and small symbols, respectively. As the four monopeptides are achiral, all minima have been represented considering the two equivalent positions: $\varphi, \psi \equiv -\varphi, -\psi$.

groups of Ac-Deg-NHMe interact with the backbone amide moieties.

Amazingly, substitution of the two α-ethyl side chains by the bulkier phenyl (Dϕg) or benzyl (Db$_z$g) groups generates an increment in the conformational flexibility. In particular, the extended ($\varphi,\psi \approx 180°, 180°$), γ-turn ($\varphi,\psi \approx -70°, 50°$), and *semi*-extended motifs were identified as minimum energy conformations for Ac-Dϕg-NHMe[36] and Ac−Db$_z$g-NHMe.[37] In both compounds the most stable arrangement is the former. A remarkable difference between the Dϕg- and Db$_z$g-containing monopeptides is found in the relative stability of the γ-turn motif. Specifically, the ΔG_{gp} of this conformation is 1.5 kcal/mol in Ac-Dϕg-NHMe while it decreases to 0.7 kcal/mol in Ac−Db$_z$g-NHMe. In contrast, the *semi*-extended conformations of Ac-Dϕg-NHMe and Ac−Db$_z$g-NHMe (φ,ψ= −42.0°, 132.6° and φ,ψ= 173.4°, −23.2°, respectively) are essentially isoenergetic with ΔG_{gp}= 2.8 and 2.7 kcal/mol, respectively. The substitution of repulsive backbone···side-chain steric contacts (i.e., N−H···CH$_2$ and N−H···CH$_3$) by attractive interactions involving the N−H groups of the amide moieties and the π-aromatic ring is responsible for the conformational differences observed among the Deg, Dϕg, and Db$_z$g monopeptides. Thus, formation of attractive N−H···π interactions leads to an increase in the number of conformational motifs with ΔG_{gp} < 3.0 kcal/mol.

Influence of the Environment on the Geometry Relaxation of Ac-D-Abu-NHMe, Ac-D-Iva-NHMe, and Ac-Deg-NHMe. The influence of the solvent polarity in the molecular geometry of three investigated dipeptides has been evaluated by considering complete geometry optimization in aqueous solution of all the minima listed in Tables 1−3 with $\Delta G_{gp} \leq$ 1.5 kcal/mol or $\Delta G_{wat} \leq$ 1.5 kcal/mol. Thus, a total of 6, 2, and 1 conformations were reoptimized for Ac-D-Abu-NHMe, Ac-D-Iva-NHMe and Ac-Deg-NHMe, respectively. Results, which are summarized in Table 4, indicate that the influence of the solvent-induced geometry relaxation in the relevant conformational parameters and relative stability of the different structures is very small. Thus, the variation of the dihedral angles with respect to the values derived from geometry optimizations in the gas-phase was smaller than 8° for all the minima with

Table 4. Values for the Representative Dihedral Angles (in deg) of Ac-D-Abu-NHMe, Ac-D-Iva-NHMe, and Ac-Deg-NHMe in the Minimum Energy Conformations Obtained from Complete Geometry Optimizations in Aqueous Solution with Free Energies in the Aqueous Solution at 298 K (ΔG_{wat}, in kcal/mol) Obtained from Complete Geometry Optimization in Aqueous Solution and Single Point Calculations Using the Gas-Phase Geometries Displayed for Comparison

conformation	φ	ψ	χ_1/χ_2[a]	ΔG_{wat} compl. optim.	ΔG_{wat} single point
			Ac-D-Abu-NHMe		
γ_D-t	85.3	−78.3	169.2	2.0	3.1
γ_D-g$^+$	85.5	−70.8	65.1	1.8	2.5
β_{DL}-g$^-$	152.9	−164.4	−63.5	1.3	0.5
β_{DL}-t	146.1	−138.0	175.5	1.0	0.7
β_{DL}-g$^+$	127.7	−144.0	64.2	0.9	0.0
α_D-g$^+$	112.8	7.1	65.4	0.0[b]	0.1
			Ac-D-Iva-NHMe		
β_{DL}-g$^-$	179.8	−179.6	−58.5	0.9	0.7
α_D-t	59.6	39.8	−176.5	0.0[c]	0.0
			Ac-Deg-NHMe		
β_{DL}-g$^-$g$^+$	180.0	180.0	−59.1/-59.2	*d*	–

[a]The dihedral angle χ_2 is only possible for Ac-Deg-NHMe. [b]G_{wat} = −535.058898 au. [c]G_{wat} = −574.342443 au. [d]G_{wat} = −613.632084 au.

exception of the α_D-g$^+$ for Ac-D-Abu-NHMe, which showed a reduction in φ of 17.2°. On the other hand, the relative stability in water predicted by single point calculations (Tables 1−3) remains practically identical to that obtained from geometry optimizations in solution. Moreover, the ΔG_{wat} values obtained using such two approaches differ by less than 1.1 kcal/mol. The overall of these results corroborate that conclusions reached in previous subsections are not altered by solvent-induced geometry relaxation effects.

CONCLUSIONS

The energy landscapes of Ac-D-Abu-NHMe, Ac-D-Iva-NHMe, and Ac-Deg-NHMe have been investigated in the gas phase and in chloroform, dichloromethane and aqueous solutions using quantum mechanical calculations at the B3LYP/6-31+G(d,p) level. Calculations on Ac-D-Abu-NHMe reveal that its conformational flexibility is similar to that expected for monopeptides of proteinogenic residues with similar chemical constitution (i.e., an aliphatic side-chain group). Thus, three backbone conformations have been identified as energetically accessible in the gas phase: γ_D, β_{DL}, and α_D. The γ-turn and extended motifs are essentially isoenergetic and more stable than the helical motif, which is disfavored by about 1.5 kcal/mol. In contrast, in aqueous solution the extended and helical structures become the only energetically accessible backbone conformations with a very similar relative stability, whereas the relative free energy of the γ-turn increases to 2.5 kcal/mol.

Substitution of the α-hydrogen atom of D-Abu by a methyl group to produce D-Iva results in remarkable conformational restrictions. For Ac-D-Iva-NHMe, the number of energetically accessible minima in the gas phase and in both chloroform and dichloromethane solution is one, while it increases to two in aqueous solution. This represents a significant decrease with respect to the eight, five, four, and four minima identified for Ac-D-Abu-NHMe in the gas phase, chloroform, dichloromethane,

dx.doi.org/10.1021/jp3045115 | J. Phys. Chem. B 2012, 116, 13297−13307

and water, respectively. The only energetically representative backbone conformation found in the gas phase, chloroform solution and dichloromethane solution for the Iva-containing monopeptide is the extended conformation. Both the helical and extended motifs are accessible in aqueous solution, even though the latter is slightly disfavored with respect to the former (by 0.7 kcal/mol). In general, the conformation profile of Iva resembles that found for Aib, the simplest $C^{\alpha,\alpha}$-dialkylated α-amino acid, which is dominated by the repulsive steric interactions between the alkyl side-chain groups and the backbone.

Finally, the conformational profile of Ac-Deg-NHMe is extremely restricted, the only energetically accessible backbone conformation in the gas phase and chloroform, dichloromethane and aqueous solutions being the extended conformation. Indeed, repulsive steric interactions between the ethyl side-chain groups and the backbone are so frequent that the conformational flexibility of the Deg-containing monopeptide has been found to be lower than that reported for other symmetric $C^{\alpha,\alpha}$-dialkylated monopeptides with bulkier side chains (e.g., Ac-Dϕg-NHMe and Ac−Db$_z$g-NHMe).

AUTHOR INFORMATION

Corresponding Author

*E-mail: carlos.aleman@upc.edu.

Notes

The authors declare no competing financial interest.

ACKNOWLEDGMENTS

This work was supported by MICINN-FEDER funds (MAT2009-09138) and by the Generalitat de Catalunya (2009SGR925 and XRQTC). Authors are indebted to the Centre de Supercomputació de Catalunya (CESCA) for computational facilities. Support for the research of C.A. was received through the "ICREA Academia".

REFERENCES

(1) Toniolo, C.; Formaggio, F.; Kaptein, B.; Broxterman, Q. B. *Synlett* **2006**, 1295−1310.

(2) Venkatraman, J.; Shankaramma, S. C.; Balaram, P. *Chem. Rev.* **2001**, *101*, 3131−3152.

(3) Toniolo, C.; Crisma, M.; Formaggio, F.; Peggion, C. *Biopolymers (Pept. Sci.)* **2001**, *60*, 396−419.

(4) Aravinda, S.; Shamala, N.; Balaram, P. *Chem. Biodivers.* **2008**, *5*, 1238−1262.

(5) Benedetti, E. *Biopolymers (Pept. Sci.)* **1996**, *40*, 3−44.

(6) Toniolo, C.; Benedetti, E. *Macromolecules* **1991**, *24*, 4004−4009.

(7) Karle, I. L.; Balaram, P. *Biochemistry* **1990**, *29*, 6747−6756.

(8) Karle, I. L.; Flippen-Anderson, J. L.; Uma, K.; Balaram, P. *Proc. Natl. Acad. Sci. U.S.A.* **1990**, *87*, 7921−7925.

(9) Bosch, R.; Jung, G.; Schmitt, H.; Winter, W. *Biopolymers* **1985**, *24*, 961−978.

(10) Gessmann, R.; Brückner, H.; Petratos, K. *J. Pept. Sci.* **2003**, *9*, 753−762.

(11) Solà, J.; Helliwell, M.; Clayden, J. *Biopolymers* **2011**, *95*, 62−69.

(12) Improta, R.; Rega, N.; Alemán, C.; Barone, V. *Macromolecules* **2001**, *34*, 7550−7557.

(13) Barone, V.; Lelj, F.; Bavoso, A.; Di Blasio, B.; Grimaldi, P.; Pavone, V.; Pedone, C. *Biopolymers* **1985**, *24*, 1759−1767.

(14) Alemán, C. *Biopolymers* **1994**, *34*, 841−847.

(15) Alemán, C.; Roca, R.; Luque, F. J.; Orozco, M. *Proteins* **1997**, *28*, 83−93.

(16) Marshall, G. R. *Intra-Science Chemistry Report*; Kharasch, N., Ed.; Gordon and Breach: New York, 1971; pp 305−316.

(17) Huston, S. E.; Marshall, G. R. *Biopolymers* **1994**, *34*, 75−90.

(18) Paterson, Y.; Rumsey, S. M.; Benedetti, E.; Némethy, G.; Scheraga, H. A. *J. Am. Chem. Soc.* **1981**, *103*, 2947−2955.

(19) Toniolo, C.; Benedetti, E. *Molecular Conformation and Biological Interactions*; Balaram, P., Ramaseshan, S., Eds., Indian Academy of Sciences: Bangalore, India, 1991; pp 497−502.

(20) Benedetti, E.; Di Blasio, B.; Pavone, V.; Pedone, C.; Toniolo, C.; Crisma, M. *Biopolymers* **1992**, *32*, 453−456.

(21) Crisma, M.; Formaggio, F.; Moretto, A.; Toniolo, C. *Biopolymers (Pept. Sci.)* **2006**, *84*, 3−12.

(22) Di Blasio, B.; Pavone, V.; Lombardi, A.; Pedone, C.; Benedetti, E. *Biopolymers* **1993**, *33*, 1037−1049.

(23) Toniolo, C. *CRC Crit. Rev. Biochem.* **1980**, *9*, 1−44.

(24) Cung, M. T.; Marraud, M.; Néel, J. *Ann. Chim. (Paris)* **1972**, 183−209.

(25) Formaggio, F.; Crisma, M.; Peggion, C.; Moretto, A.; Venanzi, M.; Toniolo, C. *Eur. J. Org. Chem.* **2012**, 167−174.

(26) Formaggio, F.; Crisma, M.; Ballano, G.; Peggion, C.; Venanzi, M.; Toniolo, C. *Org. Biomol. Chem.* **2012**, *10*, 2413−2421.

(27) Benedetti, E.; Pedone, C.; Pavone, V.; Di Blasio, B.; Saviano, M.; Fattorusso, R.; Crisma, M.; Formaggio, F.; Bonora, G. M.; Toniolo, C.; Kaczmarek, K.; Redlinski, A. S.; Leplawy, M. T. *Biopolymers* **1994**, *34*, 1409−1418.

(28) Benedetti, E.; Barone, V.; Bavoso, A.; Di Blasio, B.; Lelj, F.; Pavone, V.; Pedone, C.; Bonora, G. M.; Toniolo, C.; Leplawy, M. T.; Kaczmarek, K.; Redlinski, A. *Biopolymers* **1988**, *27*, 357−371.

(29) Toniolo, C.; Bonora, G. M.; Bavoso, A.; Benedetti, E.; Di Blasio, B.; Pavone, V.; Pedone, C.; Barone, V.; Lelj, F.; Leplawy, M. T.; Kaczmarek, K.; Redlinski, A. *Biopolymers* **1988**, *27*, 373−379.

(30) Tanaka, M.; Imawaka, N.; Kurihara, M.; Suemune, H. *Helv. Chim. Acta* **1999**, *82*, 494−510.

(31) Toniolo, C.; Benedetti, E. *Trends Biochem. Sci.* **1991**, *16*, 350−353.

(32) Torras, J.; Zanuy, D.; Crisma, M.; Toniolo, C.; Bertran, O.; Alemán, C. *Biopolymers (Pept. Sci.)* **2008**, *90*, 695−706.

(33) Revilla-López, G.; Torras, J.; Curcó, D.; Casanovas, J.; Calaza, M. I.; Zanuy, D.; Jiménez, A. I.; Cativiela, C.; Nussinov, R.; Grodzinski, P.; Alemán, C. *J. Phys. Chem. B* **2010**, *114*, 7413−7422.

(34) Revilla-López, G.; Rodríguez-Ropero, F.; Curcó, D.; Torras, J.; Calaza, M. I.; Zanuy, D.; Jiménez, A. I.; Cativiela, C.; Nussinov, R.; Alemán, C. *Proteins* **2011**, *79*, 1841−1852.

(35) Alemán, C. *J. Phys. Chem. B* **1997**, *101*, 5046−5050.

(36) Casanovas, J.; Zanuy, D.; Nussinov, R.; Alemán, C. *J. Org. Chem.* **2007**, *72*, 2174−2181.

(37) Casanovas, J.; Nussinov, R.; Alemán, C. *J. Org. Chem.* **2008**, *73*, 4205−4211.

(38) Gaussian 03, Revision B.02 Frisch, M. J.; Trucks, G. W.; Schlegel, H. B.; Scuseria, G. E.; Robb, M. A.; Cheeseman, J. R.; Montgomery, J. A.; Vreven, T., Jr.; Kudin, K. N.; Burant, J. C.; Millam, J. M.; Iyengar, S. S.; Tomasi, J.; Barone, V.; Mennucci, B.; Cossi, M.; Scalmani, G.; Rega, N.; Petersson, G. A.; Nakatsuji, H.; Hada, M.; Ehara, M.; Toyota, K.; Fukuda, R.; Hasegawa, J.; Ishida, M.; Nakajima, T.; Honda, Y.; Kitao, O.; Nakai, H.; Klene, M.; Li, X.; Knox, J. E.; Hratchian, H. P.; Cross, J. B.; Adamo, C.; Jaramillo, J.; Gomperts, R.; Stratmann, R. E.; Yazyev, O.; Austin, A. J.; Cammi, R.; Pomelli, C.; Ochterski, J. W.; Ayala, P. Y.; Morokuma, K.; Voth, G. A.; Salvador, P.; Dannenberg, J. J.; Zakrzewski, V. G.; Dapprich, S.; Daniels, A. D.; Strain, M. C.; Farkas, O.; Malick, D. K.; Rabuck, A. D.; Raghavachari, K.; Foresman, J. B.; Ortiz, J. V.; Cui, Q.; Baboul, A. G.; Clifford, S.; Cioslowski, J.; Stefanov, B. B.; Liu, G.; Liashenko, A.; Piskorz, P.; Komaromi, I.; Martin, R. L.; Fox, D. J.; Keith, T.; Al-Laham, M. A.; Peng, C. Y.; Nanayakkara, A.; Challacombe, M.; Gill, P. M. W.; Johnson, B.; Chen, W.; Wong, M. W.; Gonzalez, C.; Pople, J. A. Gaussian, Inc.: Pittsburgh, PA, 2003.

(39) Becke, A. D. *J. Chem. Phys.* **1993**, *98*, 1372−1377.

(40) Lee, C.; Yang, W.; Parr, R. G. *Phys. Rev. B* **1988**, *37*, 785−789.

(41) McLean, A. D.; Chandler, G. S. *J. Chem. Phys.* **1980**, *72*, 5639−5648.

(42) Revilla-López, G.; Torras, J.; Jiménez, A. I.; Cativiela, C.; Nussinov, R.; Alemán, C. *J. Org. Chem.* **2009**, *74*, 2403−2412.

(43) Warren, J. G.; Revilla-López, G.; Alemán, C.; Jiménez, A. I.; Cativiela, C.; Torras, J. *J. Phys. Chem. B* **2010**, *114*, 11761−11770.
(44) Revilla-López, G.; Jiménez, A. I.; Cativiela, C.; Nussinov, R.; Alemán, C.; Zanuy, D. *J. Chem. Inf. Model.* **2011**, *50*, 1781−1789.
(45) Revilla-López, G.; Laurent, A. D.; Perpete, E. A.; Jacquemin, D.; Torras, J.; Assfeld, X.; Alemán, C. *J. Phys. Chem. B* **2011**, *115*, 1232−1242.
(46) Zheng, J.; Yu, T.; Papajak, E.; Alecu, I. M.; Mielke, S. L.; Truhlar, D. G. *Phys. Chem. Chem. Phys.* **2011**, *13*, 10885−10907.
(47) MSTor: A program for calculating partition functions, free energies, enthalpies, entropies, and heat capacities of complex molecules including torsional anharmonicity ; Zheng, J.; Mielke, S. L.; Clarkson, K. L.; Truhlar, D. G. http://comp.chem.umn.edu/mstor/
(48) Tomasi, J.; Mennucci, B.; Cammi, R. *Chem. Rev.* **2005**, *105*, 2999−3094.
(49) Tomasi, J.; Persico, M. *Chem. Rev.* **1994**, *94*, 2027−2094.
(50) Miertus, M.; Scrocco, E.; Tomasi, J. *Chem. Phys.* **1981**, *55*, 117−129.
(51) Perczel, A.; Angyan, J. G.; Kajtar, M.; Viviani, W.; Rivail, J.-L.; Marcoccia, J.-F.; Csizmadia, I. G. *J. Am. Chem. Soc.* **1991**, *113*, 6256−6265.
(52) Némethy, G.; Printz, M. P. *Macromolecules* **1972**, *5*, 755−758.
(53) Matthews, B. W. *Macromolecules* **1972**, *5*, 818−819.
(54) Allen, F. H. *Acta Crystallogr.* **2002**, *B58*, 380−388.
(55) Toniolo, C.; Bonora, G. M.; Crisma, M.; Bertanzon, F.; Stevens, E. S. *Makromol. Chem.* **1981**, *182*, 3149−3162.
(56) Goodman, M.; Naider, F.; Toniolo, C. *Biopolymers* **1971**, *10*, 1719−1730.
(57) Toniolo, C.; Bonora, G. M.; Palumbo, M.; Peggion, E.; Stevens, E. S. *Biopolymers* **1978**, *17*, 1713−1727.
(58) Toniolo, C.; Bonora, G. M.; Mutter, M. *J. Am. Chem. Soc.* **1979**, *101*, 450−454.
(59) Toniolo, C.; Bonora, G. M.; Salardi, S. *Int. J. Biol. Macromol.* **1981**, *3*, 377−383.
(60) Toniolo, C.; Bonora, G. M.; Fontana, A. *Int. J. Pept. Protein Res.* **1974**, *6*, 371−380.
(61) Cocinero, E. J.; Lesarri, A.; Sanz, M. E.; Lopez, J. C.; Alonso, J. L. *ChemPhysChem* **2006**, *7*, 1481−1487.
(62) De Zotti, M.; Biondi, B.; Crisma, M.; Hjørringgaard, C. U.; Berg, A.; Brückner, H.; Toniolo, C. *Biopolymers (Pept. Sci.)* **2012**, *98*, 36−49.
(63) Bosch, R.; Brückner, H.; Jung, G.; Winter, W. *Tetrahedron* **1982**, *38*, 3579−3583.
(64) Crisma, M.; Formaggio, F.; Pantano, M.; Valle, G.; Bonora, G. M.; Toniolo, C.; Schoemaker, H. E.; Kamphuis, J. *J. Chem. Soc., Perkin Trans. 2* **1994**, 1735−1742.
(65) Crisma, M.; Moretto, A.; Rainaldi, M.; Formaggio, F.; Broxterman, Q. B.; Kaptein, B.; Toniolo, C. *J. Pept. Sci.* **2003**, *9*, 620−637.
(66) Altmann, E.; Altmann, K. H.; Nebel, K.; Mutter, M. *Int. J. Pept. Protein Res.* **1988**, *32*, 344−351.
(67) Formaggio, F.; Crisma, M.; Bonora, G. M.; Pantano, M.; Valle, G.; Toniolo, C.; Aubry, A.; Bayeul, D.; Kamphuis, J. *Pept. Res.* **1995**, *8*, 6−15.
(68) Jaun, B.; Tanaka, M.; Seiler, P.; Kühnle, F. N. M.; Braun, C.; Seebach, D. *Liebigs Ann./Rec.* **1997**, 1697−1710.
(69) Peggion, C.; Crisma, M.; Toniolo, C.; Formaggio, F. *Tetrahedron* **2012**, *68*, 4429−4433.